Heliyon 10 (2024) e29100

Contents lists available at ScienceDirect

Heliyon

journal homepage: www.cell.com/heliyon

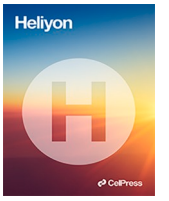

Research article

CX3CL1 and its receptor CX3CR1 interact with RhoA signaling to induce paclitaxel resistance in gastric cancer

Xiangyang Liu [1], Zhonghui Yu [1], Yun Li [*], Junzi Huang [**]

Department of Pharmaceutics, Second Affiliated Hospital of Dalian Medical University, Dalian 116027, Liaoning, PR China

ARTICLE INFO

Keywords:
CX3CL1
CX3CR1
RhoA signaling
Gastric cancer
Paclitaxel

ABSTRACT

C-X3-C motif chemokine ligand 1 (CX3CL1) is a transmembrane protein, and the membranal and soluble forms of CX3CL1 exhibit different functions, although both bind to the CX3CR1 chemokine receptor. The CX3CL1/CX3CR1 axis induces many cellular responses relevant to cancer, such as proliferation, migration, invasion, and apoptosis resistance. Here we attempt to elucidate whether CX3CL1/CX3CR1 is associated with paclitaxel (PTX) resistance in gastric cancer (GC). The Gene Expression Omnibus database was queried to screen for differentially expressed genes in GC cells caused by drug resistance, and CX3CL1 was selected as a candidate. CX3CL1 was overexpressed in PTX-resistant cells and tissues. CX3CL1 loss sensitized GC cells to PTX, promoted apoptosis and DNA damage, and inhibited cell proliferation, migration, and invasion. CX3CR1 reversed the ameliorative effect of CX3CL1 silencing on PTX sensitivity in GC cells. The promotion of PTX resistance by CX3CL1/CX3CR1 was inhibited by impairment of the small GTPase Ras homolog gene family member A (RhoA) pathway *in vitro* and *in vivo*. These findings indicate that the CX3CL1/CX3CR1 expedites PTX resistance through the RhoA signaling in GC cells.

1. Introduction

Gastric cancer (GC) contributes significantly to cancer-related deaths [1]. The prognosis of patients with GC remains poor in China, with a 5-year survival rate of 35.9% from 2010 to 2014 [2]. The standard curative therapy for GC is surgical resection, which is not possible when patients are diagnosed at an advanced stage [3]. Advanced GC patients can benefit from chemotherapeutic agents, including adriamycin, platinum drugs, 5-fluorouracil, vincristine, and paclitaxel (PTX), while primary or acquired drug resistance ultimately results in treatment failure and unsatisfactory outcomes in these patients [4]. PTX is active against a set of tumor types, and paclitaxel monotherapy has produced substantial advances in tumor response and prognosis [5]. Therefore, an improved understanding of the mechanism of PTX resistance may offer new tools for GC therapy.

Chemokines are the largest group of cytokines and can be divided into the following four groups: the CC chemokines, the CXC chemokines, C chemokines, and the CX3C chemokine [6]. CX3CL1 (also referred to as Fractalkine), the only member of the CX3C family, has a separation of three amino acid residues in its amino-terminal cysteine motif and the peculiarity of being expressed as an

* Corresponding author. Department of Pharmaceutics, Second Affiliated Hospital of Dalian Medical University, No. 467, Zhongshan Road, Hekou District, Dalian 116027, Liaoning, PR China.

** Corresponding author. Department of Pharmaceutics, Second Affiliated Hospital of Dalian Medical University, No. 467, Zhongshan Road, Hekou District, Dalian 116027, Liaoning, PR China.

E-mail addresses: liyun_273@163.com (Y. Li), huangjunziii@126.com (J. Huang).

[1] Xiangyang Liu and Zhonghui Yu contributed equally to this work.

https://doi.org/10.1016/j.heliyon.2024.e29100
Received 18 August 2023; Received in revised form 29 March 2024; Accepted 31 March 2024
Available online 1 April 2024

anchored transmembrane protein, with the chemokine domain bound to the top of a mucin stalk [7]. Furthermore, CX3CL1 was highly expressed at both mRNA and protein levels in most glioblastoma specimens (31/36), and the expression of CX3CL1 was inversely correlated with the overall survival of patients with glioblastoma ($p = 0.01$) [8,9]. CX3CL1 increases invasiveness and metastasis by increasing epithelial-to-mesenchymal transition (EMT) in prostate cancer cells [10]. Moreover, CX3CR1, the sole receptor of CX3CL1, is highly expressed in GC tissues and is associated with lymph node metastasis, advanced TNM stage, and large tumor size [11]. CX3CR1 is overexpressed in pancreatic cancer cells, and ectopic expression of CX3CL1 augments glucose uptake and lactate secretion [12]. Nevertheless, the function of the CX3CL1/CX3CR1 axis in regulating resistance, particularly PTX resistance, remains to be elucidated. The interaction between CX3CL1/CX3CR1 and the small GTPase Ras homolog gene family member A (RhoA) signaling pathway has been clarified in monocytes/macrophages [13]. RhoA signaling has been suggested to regulate the DNA damage response and its traditional function in manipulating cell morphology [14]. Collectively, we hypothesized that CX3CL1/CX3CR1 could enhance PTX resistance in GC by activating RhoA signaling. To verify this hypothesis, we examined the impact of CX3CL1/CX3CR1 on PTX resistance and RhoA signaling activation in GC. This study aimed to determine the function of CX3CL1/CX3CR1 in PTX resistance in GC and elucidate the mechanism involved.

2. Materials and methods

2.1. Specimens

Tissues from patients who underwent PTX treatment at the Second Affiliated Hospital of Dalian Medical University were enrolled in the study. The inclusion criteria were: (1) patients who were diagnosed with GC for the first time at the Second Affiliated Hospital of Dalian Medical University; (2) patients with complete clinical data; (3) patients who received PTX treatment. Exclusion criteria: (1) patients with Siewert type I esophagogastric junctional squamous carcinoma; (2) those who did not undergo surgery due to incomplete or unsuccessful PTX treatment; (3) those who combined with other malignant tumors. A total of 49 patients were enrolled for analysis, of which 18 patients showed disease progression within 6 months after the last PTX administration and the remaining 31 patients did not show disease progression. Eighteen patients who developed disease progression were included in the PTX-resistant group, and 18 patients from 31 patients who did not develop disease progression were selected by random number method for inclusion in the PTX-sensitive group. Table 1 shows the baseline characteristics of the patients with GC. Tissues were obtained after chemotherapy, frozen in liquid nitrogen, and stored at −80 °C for further studies. This study was approved by the Second Affiliated Hospital of Dalian Medical University (approval no. 20180501), and written informed consent was obtained from all patients.

2.2. Bioinformatics analysis

We selected three datasets GSE58118, GSE31811, and GSE77346 containing drug-resistant and non-drug-resistant GC samples from the Gene Expression Omnibus (GEO) database. Analysis was performed on the in-house GEO2R software (version information: R 3.2.3, Biobase 2.30.0, GEOquery 2.40.0, limma 3.26.8) with a significance threshold of 0.05 to obtain volcano plots of differentially expressed genes. The differentially expressed genes in the three GEO datasets were intersected, followed by functional clustering analysis of protein functions using String (https://cn.string-db.org/) and protein-protein interaction (PPI) network development using Cytoscape_v3.10.0.

The prognostic value of CX3CL1 and CX3CR1 (also called V28) in GC was queried on the Kaplan-Meier Plotter website (http://kmplot.com/analysis/index.php?p=service).

Table 1
Baseline characteristics of GC patients.

	PTX-sensitive patients (n = 18)	PTX-resistant patients (n = 18)
Sex, n (%)		
Male	7 (39%)	9 (50%)
Female	11 (61%)	9 (50%)
Age, median (range)	45 (33–68)	51 (32–68)
Primary tumor site, n (%)		
Cardia (n = 8)	6 (33%)	2 (11%)
Body (n = 21)	10 (56%)	11 (61%)
Antrum (n = 7)	2 (11%)	5 (28%)
Body mass index, mean (SD)	20.8 (3.5)	20.3 (3.2)
Prior radiotherapy, n (%)	7 (39%)	9 (50%)
Lymph node metastases, n (%)		
Yes	11 (61%)	12 (67%)
No	7 (39%)	6 (33%)
TNM stage, n (%)		
I~II	8 (44%)	5 (28%)
III~IV	10 (56%)	13 (72%)

Note: GC, gastric cancer; PTX, paclitaxel; SD, standard deviation; TNM, tumor, node, metastases.

2.3. Cell culture

GC cells AGS (catalog number: HTX1739, RRID: CVCL_0139) and GT38 (catalog number: HTX2611, RRID: CVCL_C8NH; both from Otwo Biotech, Shenzhen, Guangdong, China) were cultured in DMEM (Thermo Fisher Scientific Inc., Waltham, MA, USA) plus 10% FBS and 1% penicillin-streptomycin (both from Thermo Fisher) with 5% CO_2 at 37 °C.

PTX-resistant GC cells were established by exposure to increasing doses of PTX (KGA8221, KeyGen, Nanjing, Jiangsu, China). AGS and GT38 cells at the logarithmic growth phase were incubated with a complete culture medium containing PTX (2 nM) for 48 h. After that, the medium was replaced with a fresh culture medium until the cell survival rate was ≥90%. Then, the next gradient of drug resistance induction was performed, with 2 nM paclitaxel added in successive increments. The PTX-resistant cell lines AGS/PTX and GT38/PTX were obtained by culturing cell lines tolerant to 20 nM and maintaining them in a complete culture medium containing 2 nM PTX.

CX3CL1 [NM_002996.6] overexpression plasmid (pRP[Exp]-EGFP/Puro-CAG > hCX3CL1), shRNA of CX3CL1 (pPB[shRNA]-EGFP: T2A: Puro-U6>hCX3CL1), CX3CR1 [NM_001171174.1] overexpression expression plasmid (pRP[Exp]-EGFP/Puro-CAG > hCX3CR1), shRNA for CX3CR1 (pPB[shRNA]-EGFP:T2A: Puro-U6>hCX3CR1), and the respective controls used for transfection were procured from VectorBuilder (Guangzhou, Guangdong, China). Lipofectamine 3000 was used for all transfections. Cells in 96-well plates (1×10^4 cells/well) were added with 10 μL of the plasmid-lipid complex containing 100 ng of plasmid per well. When shRNA and overexpression plasmid were co-transfected, the transfection was performed using 30 pmol (~0.6 μg) shRNA + 1 μg overexpression DNA plasmid. The cells were cultured at 37 °C for 48 h, and EGFP fluorescence was observed microscopically (overexpression efficiency reached above 90%). Then, mRNA expression changes in the cells were measured using RT-qPCR. The shRNA sequences used for transfection (with CTCGAG as the loop sequence) were sh-CX3CR1 (GCGCTCAGTCCACGTTGATTTCTCGAGAAATCAACGTGGACTGAGCGC) and sh-CX3CL1 (CCCGGAGCTGTGGTAGTAATTCTCGAGAATTACTACCACAGCTCCGGG).

Cells in the 96-well plate (1×10^4 cells/well) were treated with the complete medium containing 2 μg/mL of RhoA inhibitor (CT04, Cytoskeleton, Denver, CO, USA), 0.32 nM CX3CR1 inhibitor (JMS-17-2, HY-123918, MedChemExpress, Monmouth Junction, NJ, USA) or the negative control distilled water treatment (named NC-RhoA or NC-CX3CR1) for 48 h.

2.4. RT-qPCR

Trizol (Invitrogen Inc., Carlsbad, CA, USA) was used for total RNA extraction, followed by assessment using a NanoDrop ND-1000 spectrophotometer (Thermo Fisher). Each sample was reverse transcribed to cDNA using the Prime Script™ RT reagent kit with a gDNA Eraser (Perfect Real Time) kit (Takara Biotechnology Ltd., Dalian, Liaoning, China). The relative transcription of genes was assessed using the TB Green® Premix Ex Taq™ II kit (Takara). The sense and the antisense primers were 5′-ACAGCACCACGGTGTGACGAAA-3′ and 5′-AACAGCCTGTGCTGTCTCGTCT-3’ (CX3CL1); 5′-CACAAAGGAGCAGGCATGGAAG-3′ and 5′-CAGGTTTCTCTGTAGACACAAGGC-3’ (CX3CR1); 5′-CACCATTGGCAATGAGCGGTTC-3′ and 5′-AGGTCTTTGCGGATGTCCACGT-3’ (β-actin). The mRNA expression was calculated using the $2^{-\Delta\Delta Ct}$ method and normalized to β-actin.

2.5. Chemoresistance assay

The MTT assay was implemented to evaluate PTX resistance. First, the cells were seeded into 96-well plates (5000 cells/well) and cultured in 100 μL of complete medium containing different doses of PTX for 48 h and with 20 μL MTT (5 mg/mL, Thermo Fisher) for 4 h. DMSO (150 μL, Thermo Fisher) was supplemented. The OD value of the cells at 490 nm was assessed using a microplate reader. A relative survival curve was plotted to measure the median inhibition concentration (IC_{50}).

2.6. ELISA

CX3CL1 ELISA Kit (ab192145, Abcam, Cambridge, UK) was used to detect CX3CL1 secretion in GC cell supernatants, and all operations were performed according to the manufacturer’s protocol.

2.7. Colony formation assay

Cells were treated with PTX at $IC_{50}/2$ concentrations (AGS/PTX: 15.3 nM, GT38/PTX: 14.3 nM), after which 1000 cells were seeded in six-well plates and cultured with 2 mL complete medium (refreshed at an interval of 3 days) for 14 d at 37 °C in a 5% CO_2 incubator. The colonies were fixed with 4% paraformaldehyde for 15 min, stained with crystal violet for 15 min, and evaluated under a light microscope (Zeiss, Oberkochen, Germany).

2.8. Scratch assay

Cells were seeded in 24-well cell culture plates at 1×10^5 cells/well, supplemented with 500 μL complete medium, and incubated until an 80%–90% confluence. Equally spaced scratches were created with a sterile pipette. Subsequently, 500 μL complete medium containing PTX with $IC_{50}/2$ concentrations (AGS/PTX: 15.3 nM, GT38/PTX: 14.3 nM) was added to individual wells and incubated, followed by imaging at 0 and 48 h under an inverted microscope (Leica Microsystems GmbH, Wetzlar, Germany). The results were quantified as initial scratch width - final scratch width)/initial scratch width × 100% using ImageJ software (NIH, Bethesda, MD, USA).

2.9. Transwell assays

Transwell assays were conducted using 6.5-mm transwell inserts (Millipore Corp, Billerica, MA, USA) coated (invasion assays) or uncoated with Matrigel (migration assay). Cells (5×10^5) treated with PTX at $IC_{50}/2$ concentration (AGS/PTX: 15.3 nM, GT38/PTX: 14.3 nM) for 48 h were suspended in 200 μL serum-free DMEM were plated in the apical chambers. DMEM containing 15% FBS (600 μL) was loaded into the basolateral chamber. After 24 h, the migrated or invaded cells were fixed with 50% methanol and stained with 0.5% crystal violet at room temperature for 10 min. The numbers of invaded and migrated cells were evaluated by randomly selecting five fields of view under a light microscope (Zeiss).

2.10. Apoptosis assay

GC cell apoptosis was determined using an Annexin V-FITC/PI double-stained Apoptosis Detection Kit (KeyGen Biotech). AGS/PTX and GT38/PTX cells treated with PTX at $IC_{50}/2$ concentrations (AGS/PTX: 15.3 nM, GT38/PTX: 14.3 nM) were washed with pre-chilled PBS (Invitrogen) and centrifuged at 200 g for 5 min to discard the supernatant. The cells (5×10^4 cells) were resuspended with 195 μL Annexin V-FITC conjugate and treated with 5 μL Annexin V-FITC for 10 min at room temperature in the dark. After 5-min centrifugation at 200*g*, the cells were resuspended with 190 μL Annexin V-FITC conjugate and ice-bathed with 10 μL PI staining solution for 5 min in the dark. For calculation, the cells were observed on FACSCalibur (BD Biosciences, San Jose, CA, USA).

2.11. DNA damage detection

The HCS DNA Damage Kit (Invitrogen) was used to measure the yield of DNA DSB in cells. The seeded cells were treated for 48 h with $IC_{50}/2$ concentrations of PTX (AGS/PTX: 15.3 nM, GT38/PTX: 14.3 nM), respectively. After that, the GC cells were fixed, permeabilized, stained for nuclei (DAPI; in blue) and unrepaired DNA damage (γ-H2AX; in red), and sealed with 90% glycerol. Finally, images were captured under an Olympus AX70 fluorescence microscope, and the relative fluorescence intensity of γ-H2AX was measured by Image J.

2.12. Western blot analysis

The Whole Protein Extraction Kit (KGP250, KeyGen) was used for total protein extraction, followed by quantification using the BCA method (PA115, TIANGEN Biotech Co., Ltd., Beijing, China). The extracted protein (40 μg) was mixed with the loading buffer, denatured, and subjected to polyacrylamide gel electrophoresis. The gel was blotted onto an NC membrane. The membrane was stained with Lithin Red and sealed with 8% skim milk. The target proteins were evaluated with antibodies against CX3CL1 (1:1,000, ab25088, Abcam), CX3CR1 (1:1,000, PA1-28839, Thermo Fisher), and the internal control β-actin (1:1000, ab115777, Abcam) overnight at 4 °C before a 1-h re-probing with goat anti-rabbit IgG (1:10000, A32731, Thermo Fisher) at room temperature for 2 h. The membranes were developed by ECL kit (ab65623, Abcam), and quantified using quantity one.

2.13. Tumor growth assay in vivo

The animal experimental procedures were approved by the Animal Ethics Committee of the Second Affiliated Hospital of Dalian Medical University (approval no. 20211208), and their care followed institutional guidelines. To reduce unnecessary animal sacrifice (following the 3R principle), only the AGS/PTX cells were used for *in vivo* experiments.

Thirty 4-week-old male BALB/C nude mice were purchased from Vital River (Beijing, China). Lentiviral-encapsulated sh-NC, sh-CX3CL1, and pCAG-CX3CR1 were used to infect AGS/PTX cells with a viral titer of 10^9 TU/mL, and stably infected cells were screened by puromycin. Stably infected AGS/PTX cells (sh-NC, sh-CX3CL1, sh-CX3CL1 + pCAG-CX3CR1) were injected into mice subcutaneously ($n = 10$). On day 7 after injection, PBS was given intraperitoneally to five mice in each group (NC-RhoA treated), while the remaining 5 mice were injected with Inh-RhoA at 10 mg/kg. All mice received an intraperitoneal injection of 3 mg/kg PTX. PBS, Inh-RhoA, and PTX were given at an interval of 4 days. Tumor volume was evaluated after the first injection and every 4 days for the next 20 days by the formula ($width^2 \times length$)/2. The mice were euthanized, and the tumors were harvested and weighed.

2.14. Statistical analyses

All data are presented as the mean ± SD of at least three repeated experiments. Multiple comparisons were conducted using one-way or two-way ANOVA, followed by Tukey's test. All analyses were done with GraphPad Prism 8.0 (GraphPad Software Inc., CA, United States), and significance was accepted at $p < 0.05$.

3. Results

3.1. CX3CL1 and CX3CR1 expression is upregulated in GC and associated with unsatisfactory prognosis

Differentially expressed genes caused by drug resistance in GC were filtered using the GSE58118 (gemcitabine resistance), GSE31811 (cisplatin and docetaxel combination chemotherapy), and GSE77346 (trastuzumab resistance) datasets in the GEO database

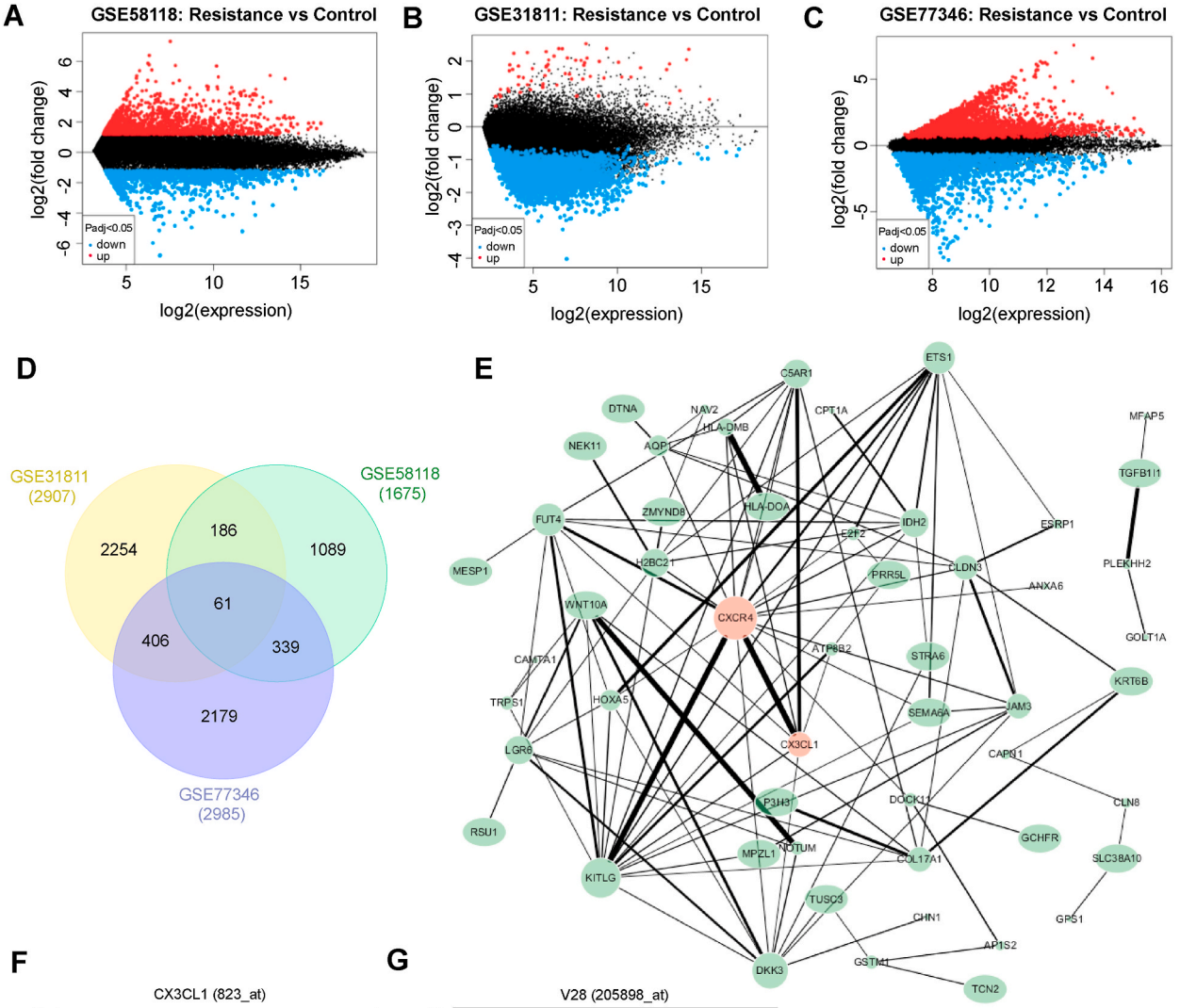

(caption on next page)

Fig. 1. Differentially expressed genes related to drug resistance in GC. (A) Differentially expressed genes in gemcitabine-resistant GC cells in the GSE58118 dataset. (B) Differentially expressed genes in cisplatin- and docetaxel-resistant GC cells in the GSE31811 dataset. (C) Differentially expressed genes in trastuzumab-resistant GC cells in the GSE77346 dataset. (D) The intersection of differentially expressed genes from the three GEO datasets yielded 61 intersecting genes closely associated with drug resistance. (E) The protein-protein interaction network reveals the interactions between 61 intersecting genes where the thickness of the lines represents the level of the combined score, and the size of the node protein represents the level of protein node degree. (F) Kaplan-Meier Plotter database analysis of the prognostic significance of CX3CL1 expression on the overall survival of GC patients. (G) Kaplan-Meier Plotter database analysis of the prognostic significance of CX3CR1 (also called V28) expression on the overall survival of GC patients. GC, gastric cancer; GEO, Gene Expression Omnibus; CX3CL1, C-X3-C motif chemokine ligand 1; CX3CR1, CX3C chemokine receptor 1.

to screen for differential expression of genomes in GC caused by drug resistance (Fig. 1A–C). A total of 61 differentially expressed genes were in the intersection (Fig. 1D). Functional clustering analysis of protein functions of the intersecting genes was conducted in String. The thickness of the lines in the PPI network was set to represent the combined score, and the size of the nodes represented the protein node degree using Cytoscape_v3.10.0 (Fig. 1E). The one with the highest protein node degree is CXCR4, and it has the highest combined score with CX3CL1.

CXCR4 has been reported to potentiate 5-Fluorouracil resistance in GC cells [15]. CX3CL1, an inflammatory chemokine with a single receptor CX3CR1, has been revealed to have a pro-tumorigenic and pro-metastatic role in a large repertoire of solid malignancies [16]. However, the effect of CX3CL1 and CX3CR1 on drug resistance in GC is still unclear. CX3CL1 and CX3CR1 (V28) expression levels in GC were both correlated with unsatisfactory prognosis of patients in the Kaplan-Meier Plotter database (Fig. 1F and G).

3.2. CX3CL1 and CX3CR1 exhibit upregulated expression in PTX-resistant GC tissues

The expression profile of CX3CL1 and CX3CR1 in frozen tissues of GC patients sensitive (n = 18) or resistant (n = 18) to PTX was detected (Fig. 2A and B). CX3CL1 and CX3CR1 expression was promoted in tumor tissues compared to the adjacent tissues and enhanced in the PTX-resistant group relative to the PTX-sensitive group. This suggests that CX3CL1 and CX3CR1 may be the regulators of PTX resistance. By gradient concentration of PTX exposure, the degree of resistance of GC cells to PTX gradually increased, and the cells at passage 8 were used as PTX-resistant cells for subsequent experiments (Fig. 2C).

RT-qPCR and Western blot analysis were also implemented to assess the expression of CX3CL1 and CX3CR1 in both parental cells and PTX-resistant cells (named AGS/PTX and GT38/PTX thereafter). CX3CL1 and CX3CR1 were remarkably elevated in AGS/PTX and GT38/PTX cells (Fig. 2D and E). We examined the expression of CX3CL1 in cell culture supernatants by ELISA and observed that the secretion of CX3CL1 was also significantly increased in PTX-resistant cells (Fig. 2F). Overexpression plasmids of CX3CL1 and CX3CR1 were transfected into parental cells, and the overexpression efficiency was detected by RT-qPCR (Fig. 2G). Overexpression of either CX3CR1 or CX3CL1 alone resulted in elevated IC_{50} of PTX and induced PTX resistance in GC cells (Fig. 2H). This suggests that CX3CR1/CX3CL1 signaling activation is a key factor in acquired PTX resistance in GC cells.

3.3. Depletion of CX3CL1 promotes the sensitivity of GC cells to PTX

CX3CL1 shRNA was then transfected into AGS/PTX and GT38/PTX cells, and the knockdown efficiency was detected by RT-qPCR (Fig. 3A). The shRNA-mediated knockdown of CX3CL1 also significantly reduced the CX3CL1 level released by GC cells (Fig. 3B). The IC_{50} values of PTX to cells were measured by MTT assay. The IC_{50} values of PTX were significantly reduced after CX3CL1 inhibition (Fig. 3C).

The GC cells were treated with $IC_{50}/2$ concentration of PTX for 48 h and subsequently subjected to cell biological behavior assays. In colony formation assays, inhibition of CX3CL1 significantly reduced the viability of AGS/PTX and GT38/PTX cells (Fig. 3D). Suppression of CX3CL1 significantly increased the apoptosis rate of AGS/PTX and GT38/PTX cells in the apoptosis assays (Fig. 3E). As revealed by both scratch assay and Transwell migration assay, silencing of CX3CL1 reduced the ability of AGS/PTX and GT38/PTX cells to migrate (Fig. 3F and G). Also, the silencing of CX3CL1 hampered the invaded cells (Fig. 3H). The role of CX3CL1 in PTX-induced DNA damage repair was also assessed. DNA double-strand break marker γ-H2AX (phosphorylated H2AX) was stained, and γ-H2AX levels were examined to detect unrepaired DNA damage. As we expected, more damage was observed in the sh-CX3CL1 group than in the sh-NC group (Fig. 3I).

3.4. CX3CR1 confers GC cell resistance to PTX in the presence of sh-CX3CL1

CX3CR1 overexpression plasmids were transfected into both parental and resistant cells, and RT-qPCR assays revealed that pCAG-CX3CR1 successfully promoted CX3CR1 expression in both cells, indicating that GC cells were easily transfected (Fig. 4A). To examine whether the impact of CX3CL1 on drug resistance in GC cells was dependent on CX3CR1, we co-transfected AGS/PTX and GT38/PTX cells with sh-CX3CL1 and pCAG-CX3CR1. pCAG-CX3CR1 significantly promoted CX3CR1 expression, as detected by RT-qPCR (Fig. 4B). The IC_{50} values of PTX to AGS/PTX and GT38/PTX cells were measured by MTT assay (Fig. 4C). The IC_{50} values were higher in AGS/PTX and GT38/PTX cells overexpressing CX3CR1. It indicates that overexpression of CX3CR1 reversed the ameliorating effect of CX3CL1 inhibition on PTX resistance in GC cells.

CX3CR1 remarkably enhanced the colony formation of AGS/PTX and GT38/PTX cells (Fig. 4D), whereas partially prevented cells from apoptosis (Fig. 4E). Overexpression of CX3CR1 elevated cell mobility, as evidenced by scratch assay and Transwell assays

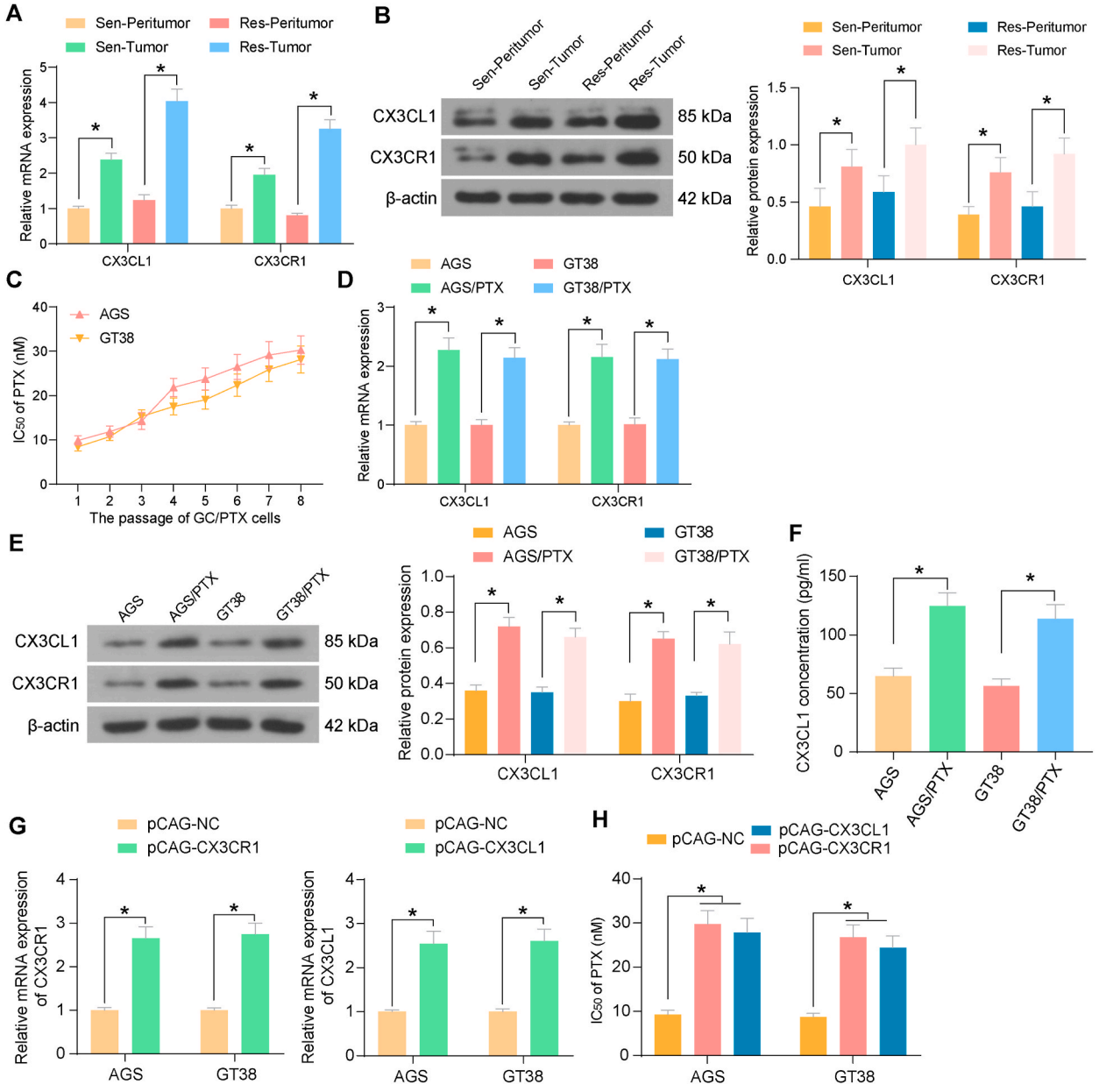

Fig. 2. CX3CL1 and CX3CR1 are upregulated in PTX-resistant GC. (A) CX3CL1 and CX3CR1 mRNA expression in tumor tissues of PTX-Sen (sensitive) or PTX-Res (resistant) GC patients using RT-qPCR. (B) Representative blots of CX3CL1 and CX3CR1 in PTX-Sen or PTX-Res GC tissues using Western blot (See the Supplementary Material 1 for all blots of 36 patients) (uncropped images of blots are provided as Supplementary material 2). (C) The IC_{50} value of PTX to GC cells after culturing with graded concentrations of PTX using MTT assays (n = 3). (D) The mRNA expression of CX3CL1 and CX3CR1 expression in parental and drug-resistant GC cells using RT-qPCR (n = 3). (E) The protein expression of CX3CL1 and CX3CR1 expression in parental and drug-resistant GC cells using Western blot (n = 3) (uncropped images of blots are provided as Supplementary material 2). (F) CX3CL1 secretion in cell culture supernatants of parental GC cells and PTX-resistant cells was analyzed using ELISA (n = 3). (G) The overexpression efficiency of CX3CL1 or CX3CR1 in parental GC cells was analyzed using RT-qPCR assay (n = 3). (H) IC_{50} value of PTX to GC cells after overexpression of CX3CL1 or CX3CR1 in parental GC cells using MTT assays (n = 3). Experiments were analyzed using two-way ANOVA followed by Tukey's post hoc test. Data are shown as mean ± SD. *$p < 0.05$. GC, gastric cancer; CX3CL1, C-X3-C motif chemokine ligand 1; CX3CR1, CX3C chemokine receptor 1, PTX, paclitaxel; IC_{50}, median inhibition concentration.

(Fig. 4F–H). In addition, we examined γ-H2AX levels in AGS/PTX and GT38/PTX cells to detect unrepaired DNA damage. DNA damage was suppressed by CX3CR1 overexpression as well (Fig. 4I). We also knocked down CX3CR1 alone in drug-resistant cells (Fig. 4J), and we observed that depletion of CX3CR1 expression effectively sensitized GC cells to PTX (Fig. 4K) and inhibited cell proliferation (Fig. 4L).

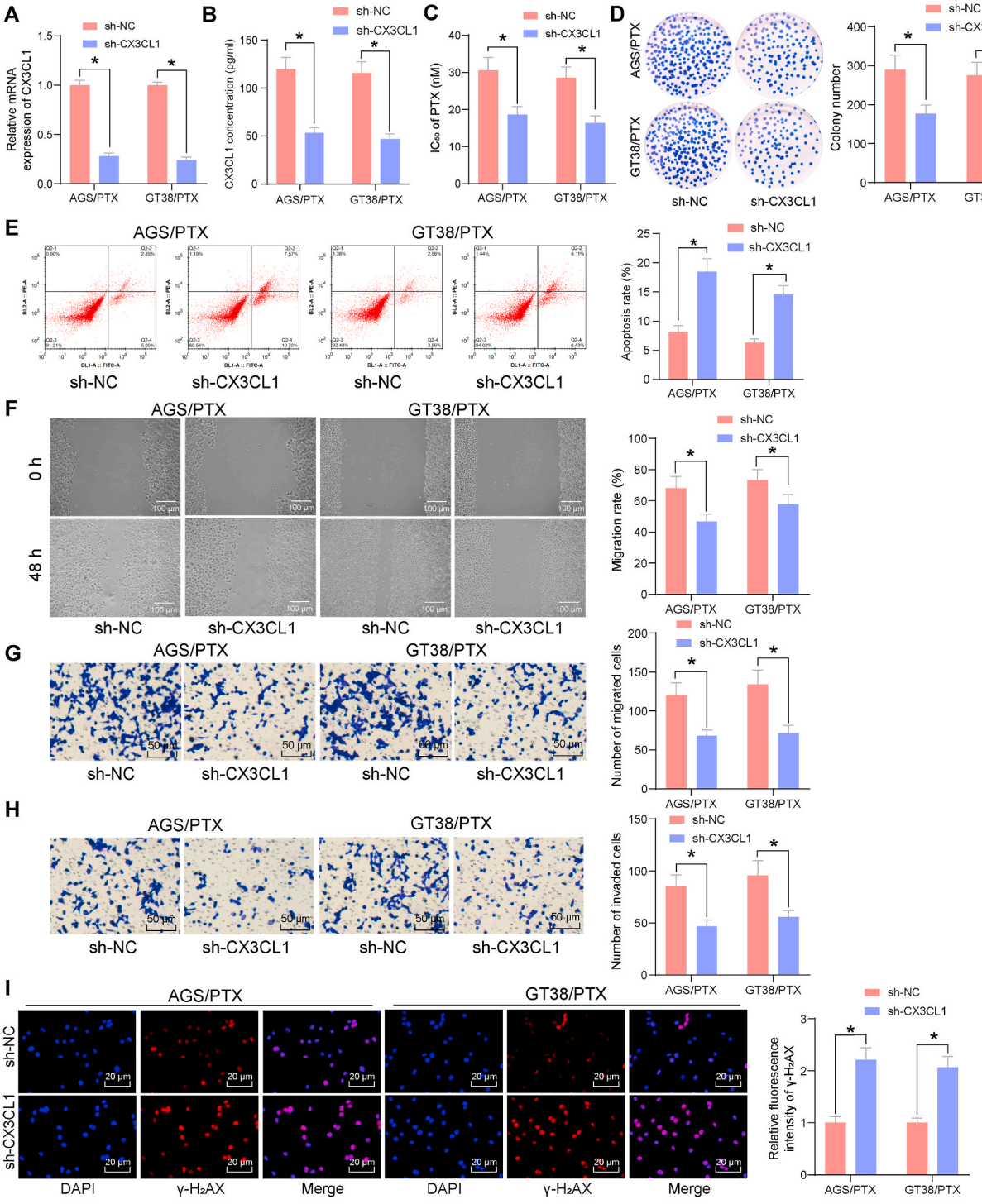

Fig. 3. Depletion of CX3CL1 promotes GC cell sensitivity *in vitro*. (A) The knockdown efficiency of sh-CX3CL1 in GC cells using RT-qPCR (n = 3). (B) CX3CL1 secretion in cell culture supernatants of PTX-resistant cells was analyzed using ELISA (n = 3). (C) The IC_{50} value of PTX to GC cells in response to sh-CX3CL1 was measured using MTT assay (n = 3). (D) The viability of cells in response to sh-CX3CL1 was measured using a colony formation assay. (E) Detection of apoptotic cells in response to sh-CX3CL1 using flow cytometry (n = 3). (F) The wound healing results of GC cells in response to sh-CX3CL1 (n = 3). (G–H) The migration and invasion abilities of GC cells in response to sh-CX3CL1 were measured using Transwell assay (n = 3). (I) γ-H2AX staining analysis of the cellular DNA damage in response to sh-CX3CL1 (n = 3). Experiments were analyzed using two-way ANOVA followed by Tukey's post hoc test. Data are shown as mean ± SD. *$p < 0.05$. GC, gastric cancer; CX3CL1, *C*-X3-C motif chemokine ligand 1; CX3CR1, CX3C chemokine receptor 1; PTX, paclitaxel; IC_{50}, median inhibition concentration.

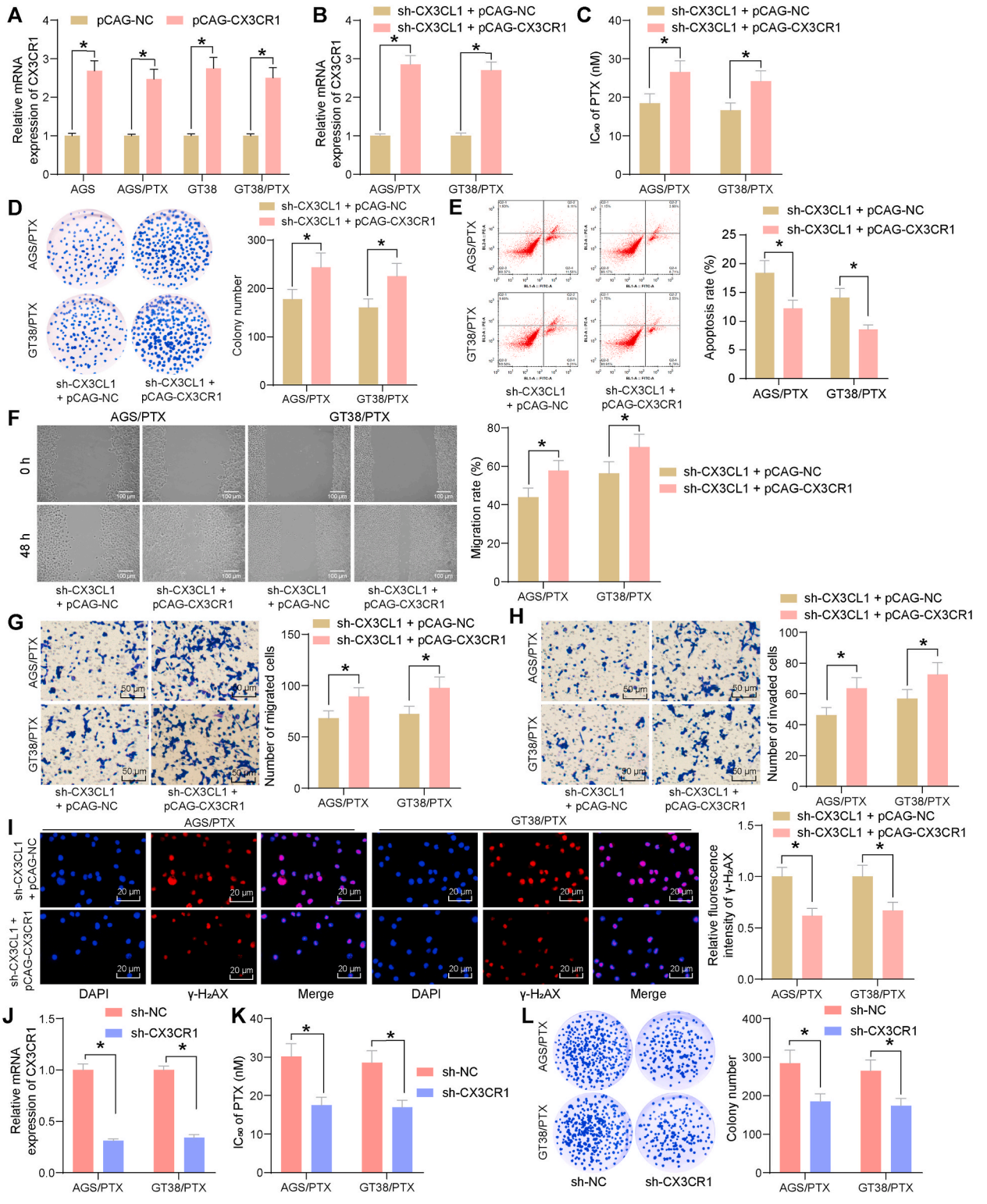

(caption on next page)

Fig. 4. CX3CR1 antagonizes the promoting effects of sh-CX3CL1 on GC cell sensitivity to PTX. (A) The overexpression efficiency of pCAG-CX3CR1 in GC cells (n = 3). (B) The effect of sh-CX3CL1 and pCAG-CX3CR1 co-transfection on CX3CR1 expression using RT-qPCR (n = 3). (C) The IC_{50} value of PTX to GC cells in response to pCAG-CX3CR1 was measured using MTT assay (n = 3). (D) The viability of cells in response to pCAG-CX3CR1 was measured using a colony formation assay (n = 3). (E) Detection of apoptotic cells in response to pCAG-CX3CR1 using flow cytometry (n = 3). (F) The wound healing results of GC cells in response to pCAG-CX3CR1 (n = 3). (G–H) The migration and invasion abilities of GC cells in response to pCAG-CX3CR1 were measured using Transwell assay (n = 3). (I) γ-H2AX staining analysis of the cellular DNA damage (n = 3). (J) The knockdown efficiency of sh-CX3CR1 using RT-qPCR (n = 3). (K) The IC_{50} value of PTX to GC cells in response to sh-CX3CR1 was measured using MTT assay (n = 3). (L) The viability of cells in response to sh-CX3CR1 was measured using colony formation assay (n = 3). Experiments were analyzed using two-way ANOVA followed by Tukey's post hoc test. Data are shown as mean ± SD. *$p < 0.05$. GC, gastric cancer; CX3CL1, C-X3-C motif chemokine ligand 1; CX3CR1, CX3C chemokine receptor 1; PTX, paclitaxel; IC_{50}, median inhibition concentration.

3.5. CX3CL1/CX3CR1 regulates the PTX resistance of GC cells through the RhoA signaling in vitro

We used an inhibitor of CX3CR1 (Inh-CX3CR1) in combination with the RhoA inhibitor to treat AGS/PTX and GT38/PTX cells and assessed the cell resistance using MTT assays (Fig. 5A). We observed that Inh-CX3CR1 treatment conferred PTX sensitivity to AGS/PTX and GT38/PTX cells, while the combined use of Inh-RhoA further inhibited the PTX resistance of the cells. The aforementioned GC cells were subjected to MTT assays. It was found that the RhoA inhibitor not only reinforced the inhibiting effect of sh-CX3CL1 on the IC_{50} value but also reversed the promoting effect of pCAG-CX3CR1 (Fig. 5B).

Besides, the clonogenic, migratory, and invasive GC cells were further reduced in the sh-CX3CL1 + Inh-RhoA group relative to the sh-CX3CL1 + NC-RhoA group, while apoptosis and DNA damage of cells were elevated (Fig. 5C–H). Relative to distilled water, the RhoA inhibitor reverted the malignant phenotype in the presence of sh-CX3CL1 + pCAG-CX3CR1 (Fig. 5C–H).

3.6. CX3CL1/CX3CR1 regulates the PTX resistance of GC cells through the RhoA signaling in vivo

The aforementioned AGS/PTX cells were subjected to injected into the axillae of nude mice, followed by Inh-RhoA and PTX treatment. We found that blockage of the RhoA signaling significantly repressed tumor formation. Moreover, the tumor suppressor effects of sh-CX3CL1 were more pronounced upon RhoA inhibitor treatment. Meanwhile, the RhoA inhibitor reversed the supporting effects of pCAG-CX3CR1 on tumor growth (Fig. 6A and B).

4. Discussion

Taxanes, including PTX, represent an imperative group of antineoplastic agents that interfere with microtubule function, contributing to changed mitosis and cellular death [15]. However, chemotherapy resistance remains a main barrier to achieving effective GC treatment. We revealed a significant augment in CX3CL1 and CX3CR1 expression in GC tissues from patients who were resistant to PTX relative to patients who were sensitive to PTX. Mechanistically, CX3CL1 depletion promoted cell apoptosis and DNA damage by binding to the CX3CR1 promoter. Moreover, the inhibitor of RhoA signaling partially sensitized GC cells to PTX *in vitro* and *in vivo* in the presence of CX3CR1. We, therefore, expounded a novel mechanism of GC chemoresistance that CX3CL1/CX3CR1 contributes to GC chemotherapy resistance by modulating DNA damage, signifying that the perturbations of the CX3CL1/CX3CR1/RhoA axis might reverse PTX resistance in GC (Fig. 7).

CX3CL1 is originally translated as a transmembrane protein but can be proteolytically processed to produce a soluble chemokine and has been demonstrated to signal via its receptor CX3CR1 [16]. More specifically, a high level of CX3CL1 has been revealed to inhibit the expression of lysosomal protein transmembrane 5, explaining how estrogen receptor-positive breast cancer metastasized to the spine [17]. Furthermore, the expression of CX3CL1 and CX3CR1 in GC tissues was higher than those in adjacent tissues and was promoted in GC tissues from the perineural invasion-positive group compared to the perineural invasion-negative group [18]. Here, we observed consistent results that CX3CL1 and CX3CR1 were remarkably elevated in tumor tissues from GC patients resistant to PTX relative to those from GC patients sensitive to PTX. Given that the secretion of soluble CX3CL1 from bone marrow endothelial cells was promoted by ADAM17 in hepatocellular carcinoma [19], ELISA was conducted to verify the impact of soluble CX3CL1 on PTX resistance GC. It was found that CX3CL1 release was more pronounced in PTX-resistant GC cells and knockdown of CX3CL1 using shRNA also reduced its overproduction. The development of cancer drug resistance includes increased drug efflux, induction of anti-apoptosis mechanisms, alterations in the tumor microenvironment, and boosted DNA repair [20]. In the study here, we found that loss of CX3CL contributed to enhanced DNA damage, which might partially explain the mechanism for overcoming drug resistance. Additionally, CX3CR1 expression was associated with cellular migration *in vitro* and tumor metastasis of clear cell renal cell carcinoma *in vivo* [21]. CX3CR1 upregulation in tumor-associated macrophages was related to dismal prognosis, and in a microenvironment lacking CX3CR1, the liver metastasis of colon cancer cells was remarkably suppressed [22]. In addition to the direct evidence regarding the binding relation between CX3CL and CX3CR1 in GC cells, we also presented that overexpression of CX3CR1 successfully reversed the supporting effects of sh-CX3CL1 on GC cell sensitivity to PTX.

According to Daniel et al., binding of CXCL12 to CXCR4 and CXCR7 on tumor cells resulted in anti-apoptotic signaling via Bcl-2 and survivin upregulation, and EMT event via the Rho-ROCK pathway [23]. In cultured cardiac and renal cells, soluble CX3CL1 augmented mitochondrial-dependent apoptosis via induction of the RhoA/ROCK1-Bax signaling [24]. Likewise, exposure to CX3CL1 elevated *p*-RhoA (Ser188)/p-ROCK2 (Tyr182) levels in hepatocellular carcinoma cells [25]. These findings validated the interaction between CX3CL1 and the RhoA signaling. However, the detailed mechanism remains to be further explored. RhoA signaling has been verified to

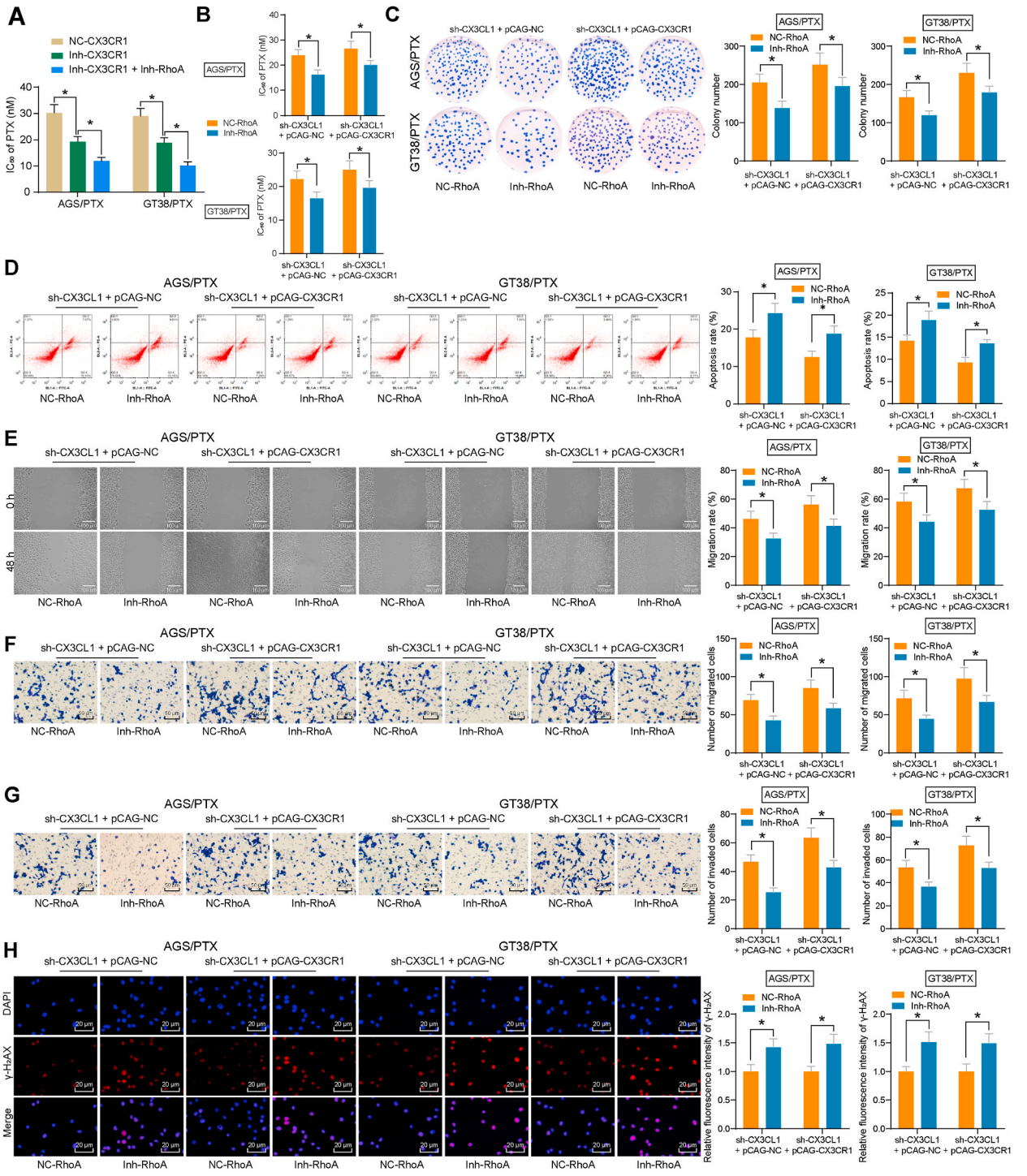

Fig. 5. Blockage of RhoA signaling rescues PTX resistance induced by CX3CR1 in GC cells. (A) The IC_{50} value of PTX to GC cells in response to the CX3CR1 inhibitor alone or with the RhoA inhibitor using MTT assays (n = 3). (B) The IC_{50} value of PTX to GC cells in response to the pCAG-NC or pCAG-CX3CR1 + RhoA inhibitor was measured using an MTT assay (n = 3). (C) The viability of cells was measured using a colony formation assay (n = 3). (D) Detection of apoptotic cells using flow cytometry (n = 3). (E) The wound healing results of GC cells (n = 3). (F–G) The migration and invasion abilities of GC cells were measured using Transwell assay (n = 3). (H) γ-H2AX staining analysis of the cellular DNA damage (n = 3). Experiments were analyzed using two-way ANOVA followed by Tukey's post hoc test. Data are shown as mean ± SD. *$p < 0.05$. GC, gastric cancer; CX3CL1, C-X3-C motif chemokine ligand 1; CX3CR1, CX3C chemokine receptor 1; RhoA, Ras homolog gene family member A; IC_{50}, median inhibition concentration.

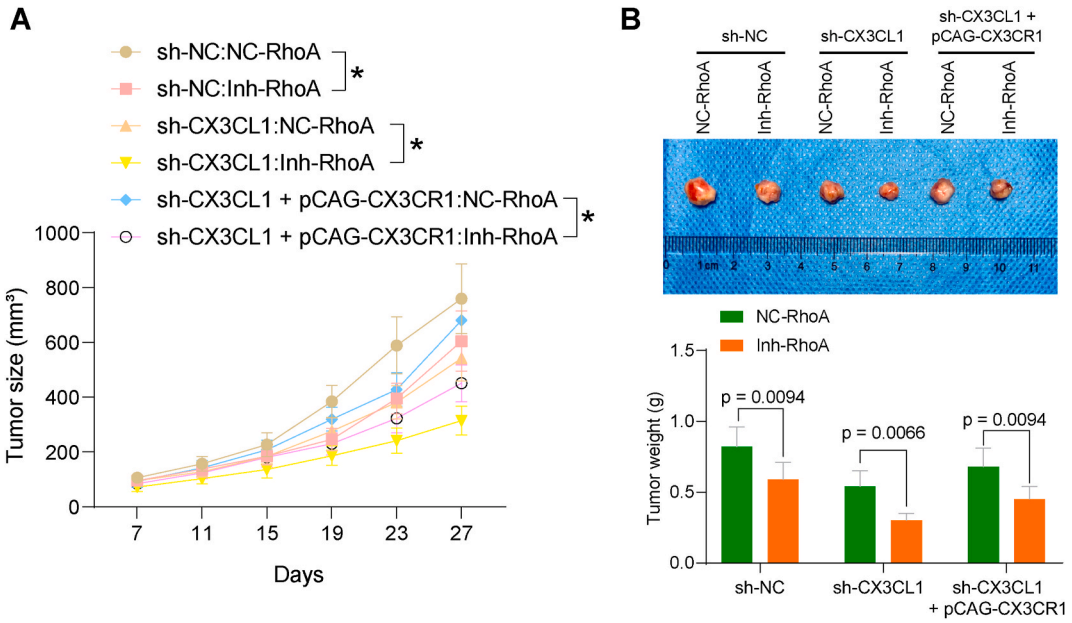

Fig. 6. RhoA inhibitor alone and depletion of CX3CL1 exert anti-tumor effects on the GC xenografts. (A–B) Tumor growth curves and tumor weights of mice (n = 5). Experiments were analyzed using two-way ANOVA followed by Tukey's post hoc test. Data are shown as mean ± SD. *$p < 0.05$. GC, gastric cancer; CX3CL1, C-X3-C motif chemokine ligand 1; RhoA, Ras homolog gene family member A.

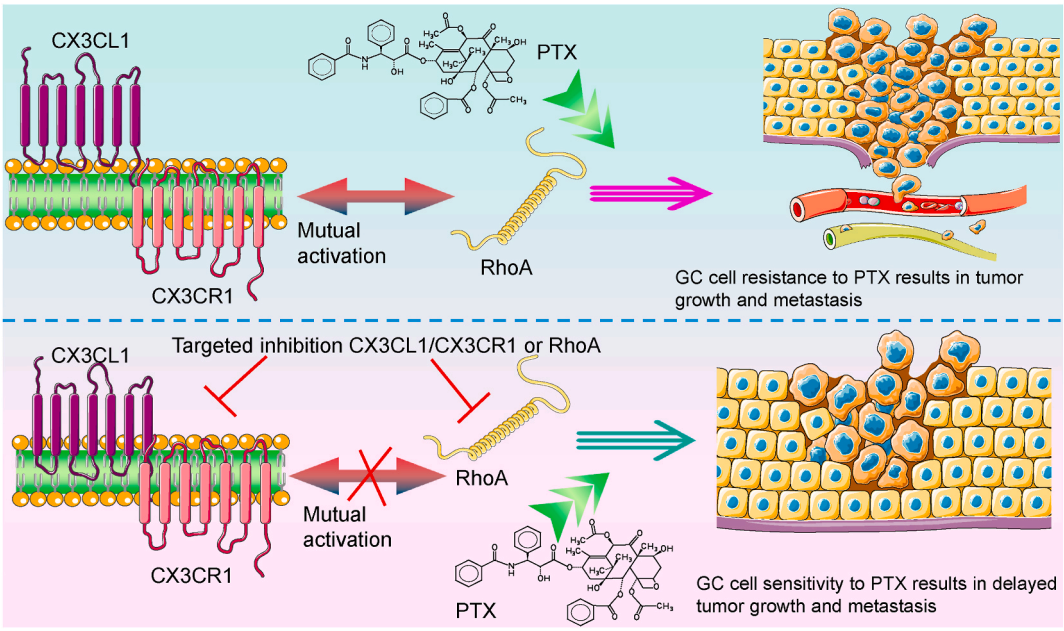

Fig. 7. Graphical summary of the mechanisms for CX3CL1/CX3CR1-induced PTX resistance in GC (plotted by Servier Medical Art licensed under a Creative Commons Attribution 3.0 Unported License, smart.servier.com). CX3CL1/CX3CR1 and RhoA mutual activation promote PTX resistance in GC cells, leading to tumor growth and metastasis. In contrast, by targeted inhibition of CX3CL1/CX3CR1 or RhoA, the mutual activation of CX3CL1/CX3CR1 and RhoA can be blocked to sensitize GC cells to PTX resistance, thereby inhibiting tumor growth and metastasis.

influence the activity of some widely used chemotherapeutics [26]. For instance, monensin synergized with chemotherapy in uveal melanoma by lowering the phosphorylation of downstream targets of RhoA signaling, including ROCK, MYPT1, and MLC, and RhoA activator calpeptin remarkably eradicated the repressive effects of monensin on RhoA activity, proliferation, migration and survival of uveal melanoma cells [25]. Our observation here indicated that suppression of RhoA using CT04 could partially reduce the expression of CX3CR1, thus impeding the GC cell resistance to PTX and their abilities to grow, migrate, and invade. Similarly, A549 cells had

weakened migration in response to the treatment with the Rho inhibitor CT04 [19]. Moreover, RhoA inhibition weakened the activity of cancer-related fibroblasts and overcame radiation resistance in pancreatic cancer [27]. Further studies are also essential to verify whether the interplay between CX3CL1/CX3CR1 and the RhoA signaling was also involved in the resistance to other chemotherapeutic agents and other types of cancers. Additional studies might be required to broaden our understanding of the RhoA signaling involvement in GC.

5. Conclusion

In summary, our results showed the CX3CL1/CX3CR1 upregulation in PTX-resistant human tissues and cells. Suppression of CX3CL1 reduced the PTX resistance and enhanced DNA damage and apoptosis of GC-resistant cells, while CX3CR1 upregulation repressed these biological functions. Furthermore, the co-dependence of the RhoA signaling and CX3CL1/CX3CR1 was necessary for the maintenance of PTX resistance. The combined and precise targeting of this axis might have therapeutic benefits in the management of PTX resistance in GC patients.

Ethics statement

This study was approved by the Second Affiliated Hospital of Dalian Medical University (approval no. 20180501) on April 27, 2018 and written informed consent was obtained from all patients. The animal experimental procedures were approved by the Animal Ethics Committee of the Second Affiliated Hospital of Dalian Medical University (approval no. 20211208) on December 3, 2021, and their care followed institutional guidelines.

Funding

None.

Data availability statement

Data will be made available on request.

CRediT authorship contribution statement

Xiangyang Liu: Writing – review & editing, Writing – original draft, Validation, Supervision, Software, Formal analysis, Data curation, Conceptualization. **Zhonghui Yu:** Writing – review & editing, Visualization, Validation, Supervision, Resources, Methodology, Data curation, Conceptualization. **Yun Li:** Writing – review & editing, Validation, Software, Resources, Investigation, Formal analysis, Data curation. **Junzi Huang:** Writing – review & editing, Visualization, Validation, Methodology, Investigation, Funding acquisition, Formal analysis.

Declaration of competing interest

The authors declare that they have no known competing financial interests or personal relationships that could have appeared to influence the work reported in this paper.

All authors read and declare no conflicts of this manuscript.

Appendix A. Supplementary data

Supplementary data to this article can be found online at https://doi.org/10.1016/j.heliyon.2024.e29100.

References

[1] N. Cancer Genome Atlas Research, Comprehensive molecular characterization of gastric adenocarcinoma, Nature 513 (7517) (2014) 202–209.
[2] L. Yang, R. Zheng, N. Wang, Y. Yuan, S. Liu, H. Li, S. Zhang, H. Zeng, W. Chen, Incidence and mortality of stomach cancer in China, 2014, Chin. J. Cancer Res. 30 (3) (2018) 291–298.
[3] J.J. Marin, R. Al-Abdulla, E. Lozano, O. Briz, L. Bujanda, J.M. Banales, R.I. Macias, Mechanisms of resistance to chemotherapy in gastric cancer, Anti Cancer Agents Med. Chem. 16 (3) (2016) 318–334.
[4] L. Wei, J. Sun, N. Zhang, Y. Zheng, X. Wang, L. Lv, J. Liu, Y. Xu, Y. Shen, M. Yang, Noncoding RNAs in gastric cancer: implications for drug resistance, Mol. Cancer 19 (1) (2020) 62.
[5] J. Sakamoto, T. Matsui, Y. Kodera, Paclitaxel chemotherapy for the treatment of gastric cancer, Gastric Cancer 12 (2) (2009) 69–78.
[6] N. Nagarsheth, M.S. Wicha, W. Zou, Chemokines in the cancer microenvironment and their relevance in cancer immunotherapy, Nat. Rev. Immunol. 17 (9) (2017) 559–572.
[7] S. Rivas-Fuentes, A. Salgado-Aguayo, J. Arratia-Quijada, P. Gorocica-Rosete, Regulation and biological functions of the CX3CL1-CX3CR1 axis and its relevance in solid cancer: a mini-review, J. Cancer 12 (2) (2021) 571–583.

[8] M. Erreni, G. Solinas, P. Brescia, D. Osti, F. Zunino, P. Colombo, A. Destro, M. Roncalli, A. Mantovani, R. Draghi, D. Levi, Y.B.R. Rodriguez, P. Gaetani, G. Pelicci, P. Allavena, Human glioblastoma tumours and neural cancer stem cells express the chemokine CX3CL1 and its receptor CX3CR1, Eur. J. Cancer 46 (18) (2010) 3383–3392.
[9] R.M. Urbantat, P. Vajkoczy, S. Brandenburg, Advances in chemokine signaling pathways as therapeutic targets in glioblastoma, Cancers 13 (12) (2021).
[10] J. Tang, L. Xiao, R. Cui, D. Li, X. Zheng, L. Zhu, H. Sun, Y. Pan, Y. Du, X. Yu, CX3CL1 increases invasiveness and metastasis by promoting epithelial-to-mesenchymal transition through the TACE/TGF-alpha/EGFR pathway in hypoxic androgen-independent prostate cancer cells, Oncol. Rep. 35 (2) (2016) 1153–1162.
[11] L.M. Wei, S. Cao, W.D. Yu, Y.L. Liu, J.T. Wang, Overexpression of CX3CR1 is associated with cellular metastasis, proliferation and survival in gastric cancer, Oncol. Rep. 33 (2) (2015) 615–624.
[12] H. Ren, T. Zhao, J. Sun, X. Wang, J. Liu, S. Gao, M. Yu, J. Hao, The CX3CL1/CX3CR1 reprograms glucose metabolism through HIF-1 pathway in pancreatic adenocarcinoma, J. Cell. Biochem. 114 (11) (2013) 2603–2611.
[13] Y. Liu, W. Chen, C. Wu, L.J. Minze, J.Z. Kubiak, X.C. Li, M. Kloc, R.M. Ghobrial, Macrophage/monocyte-specific deletion of Ras homolog gene family member A (RhoA) downregulates fractalkine receptor and inhibits chronic rejection of mouse cardiac allografts, J. Heart Lung Transplant. 36 (3) (2017) 340–354.
[14] C. Cheng, D. Seen, C. Zheng, R. Zeng, E. Li, Role of small GTPase RhoA in DNA damage response, Biomolecules 11 (2) (2021).
[15] J.A. Yared, K.H. Tkaczuk, Update on taxane development: new analogs and new formulations, Drug Des. Dev. Ther. 6 (2012) 371–384.
[16] M.S. Subbarayan, A. Joly-Amado, P.C. Bickford, K.R. Nash, CX3CL1/CX3CR1 signaling targets for the treatment of neurodegenerative diseases, Pharmacol. Ther. 231 (2022) 107989.
[17] Q. Meng, L. Zhou, H. Liang, A. Hu, H. Zhou, J. Zhou, X. Zhou, H. Lin, X. Li, L. Jiang, J. Dong, Spinespecific downregulation of LAPTM5 expression promotes the progression and spinal metastasis of estrogen receptorpositive breast cancer by activating glutaminedependent mTOR signaling, Int. J. Oncol. 60 (4) (2022).
[18] C.Y. Lv, T. Zhou, W. Chen, X.D. Yin, J.H. Yao, Y.F. Zhang, Preliminary study correlating CX3CL1/CX3CR1 expression with gastric carcinoma and gastric carcinoma perineural invasion, World J. Gastroenterol. 20 (15) (2014) 4428–4432.
[19] B. Huang, W. Luo, L. Sun, Q. Zhang, L. Jiang, J. Chang, X. Qiu, E. Wang, MiRNA-125a-3p is a negative regulator of the RhoA-actomyosin pathway in A549 cells, Int. J. Oncol. 42 (5) (2013) 1734–1742.
[20] L. Gao, Z.X. Wu, Y.G. Assaraf, Z.S. Chen, L. Wang, Overcoming anti-cancer drug resistance via restoration of tumor suppressor gene function, Drug Resist Updat 57 (2021) 100770.
[21] X. Yao, L. Qi, X. Chen, J. Du, Z. Zhang, S. Liu, Expression of CX3CR1 associates with cellular migration, metastasis, and prognosis in human clear cell renal cell carcinoma, Urol. Oncol. 32 (2) (2014) 162–170.
[22] J. Zheng, M. Yang, J. Shao, Y. Miao, J. Han, J. Du, Chemokine receptor CX3CR1 contributes to macrophage survival in tumor metastasis, Mol. Cancer 12 (1) (2013) 141.
[23] S.K. Daniel, Y.D. Seo, V.G. Pillarisetty, The CXCL12-CXCR4/CXCR7 axis as a mechanism of immune resistance in gastrointestinal malignancies, Semin. Cancer Biol. 65 (2020) 176–188.
[24] C. Zheng, W. Xuan, Z. Chen, R. Zhang, X. Huang, Y. Zhu, S. Ma, K. Chen, L. Chen, M. He, H. Lin, W. Liao, J. Bin, Y. Liao, CX3CL1 Worsens Cardiorenal Dysfunction and Serves as a therapeutic target of canagliflozin for cardiorenal syndrome, Front. Pharmacol. 13 (2022) 848310.
[25] C. Zeng, M. Long, Y. Lu, Monensin synergizes with chemotherapy in uveal melanoma through suppressing RhoA, Immunopharmacol. Immunotoxicol. 45 (1) (2023) 35–42.
[26] S. Nam, J.H. Kim, D.H. Lee, RHOA in gastric cancer: functional roles and therapeutic potential, Front. Genet. 10 (2019) 438.
[27] N. Xia, N. Yang, Q. Shan, Z. Wang, X. Liu, Y. Chen, J. Lu, W. Huang, Z. Wang, HNRNPC regulates RhoA to induce DNA damage repair and cancer-associated fibroblast activation causing radiation resistance in pancreatic cancer, J. Cell Mol. Med. 26 (8) (2022) 2322–2336.